MICHIGAN STATE UNIVERSITY

CYCLOTRON LABORATORY

SHELL-MODEL CALCULATIONS WITH A SKYRME-TYPE EFFECTIVE INTERACTION

H. SAGAWA, B.A. BROWN and O. SCHOLTEN

FEBRUARY 1985

MSUCL-511

MSUCL-511
Feb. 1985

Shell-Model Calculations with a Skyrme-type Effective Interaction

H. Sagawa, B. A. Brown, and O. Scholten

National Superconducting Cyclotron Laboratory
Michigan State University
East Lansing, MI 48824-1321

Abstract:

Shell-model calculations for the s-d shell nuclei and Sn-isotopes are performed using the Hartree-Fock wave functions and the two-body matrix elements based upon the SGII Skyrme-type density-dependent interaction. We reproduce the spectra of several nuclei from the beginning to the end of the s-d shell. The experimental pairing gaps for the Sn-isotopes are also obtained from calculations in the generalized seniority scheme using the same interaction. We find that the lower-power of the density dependence associated with the SGII interaction is essential for obtaining realistic energy spectra in this wide range of mass.

It has been a long-standing problem to establish an effective interaction which can be used both for the calculation of the saturation properties and the excitation spectra of finite nuclei. A fundamental approach is based on the reaction matrix theory [1,2]. Namely, an effective interaction is determined from the phase shifts of nucleon-nucleon scattering, and then a G-matrix calculation is carried out to obtain the two-body matrix elements for the structure calculations. However, this bare G-matrix does not give a proper account of the phenomenological two-body matrix elements. It has been pointed out [2] that the effect of core-polarization must be included in order to obtain reasonable success in the structure calculations. Since this kind of approach involves time-consuming computations, it is difficult to apply to the shell-model calculations of the open-shell and heavy nuclei.

Vautherin and Brink [3] have proposed a simple interaction, the Skyrme interaction, which has been very successful for Hartree-Fock (H-F) calculations of many nuclei. With a proper parametrization, this interaction gives satisfactory results both for the saturation properties of nuclear matter and the properties of the giant resonances. However, it is not clear whether this interaction is useful also for shell-model calculations of low-lying collective states since most previous parameter sets of the Skyrme interaction such as the SIII set show an anti-pairing effect [4].

Recently, this problem with the anti-pairing has been improved by the introduction of a density-dependent interaction with a small spin-exchange mixture [5] or the introduction of an additional parameter for the mixing of the density-dependent interaction and the three-body force [6]. One of the

advantages of the Skyrme-type interaction is that the calculations of the H-F properties and the two-body matrix elements can be carried out relatively fast. For example, the H-F calculation for ^{208}Pb takes about one minute on a VAX-780 and 332 two-body matrix elements of the (1s,1p and 1d-2s) configuration space discussed below are obtained in about three minutes.

The aim of this letter is to apply the Skyrme-type interaction to the shell-model calculations of open-shell nuclei. We use the parameter set SGII [5] in all of the following calculations. This parameter set reproduces the ground-state properties (the binding energy, the single-particle energies and the root mean square (rms) radius) and also, as will be shown below, the energy spectra. Our calculation is performed in the following way. First, the spherical H-F equation is solved to obtain the single-particle energies (s.p.e.) and radial wave functions. Next, the two-body matrix elements for the SGII interaction are calculated by using these H-F wave functions. Thus, all ingredients of our shell-model calculations are derived from the SGII interaction.

The Skyrme interaction has five types of terms. Each term is characterized by a δ-force in coordinate space which makes numerical calculations easy. The interaction is written explicitly as

$$V(\vec{r}_1,\vec{r}_2) = t_0(1+x_0P_\sigma)\delta(\vec{r}_1-\vec{r}_2) + \frac{1}{6}\,t_3(1+x_3P_\sigma)\rho^\alpha\delta(\vec{r}_1-\vec{r}_2)$$

$$+ \frac{t_1}{2}\,(1+x_1P_\sigma)(\vec{k}'^2+\vec{k}^2)\delta(\vec{r}_1-\vec{r}_2) + t_2\,(1+x_2P_\sigma)\vec{k}'\cdot\delta(\vec{r}_1-\vec{r}_2)\vec{k}$$

$$+ iW_0(\vec{\sigma}_1+\vec{\sigma}_2)\cdot\vec{k}'\times\delta(\vec{r}_1-\vec{r}_2)\vec{k} \qquad (1)$$

where $\vec{k}=(\vec{\nabla}_1-\vec{\nabla}_2)/2i$ and $\vec{k}'=-(\overleftarrow{\nabla}_1-\overleftarrow{\nabla}_2)/2i$. The parameters of SGII force are t_0=-2645 MeV·fm^3, x_0=0.09, t_1=340 MeV·fm^5, x_1=-0.0588, t_2=-41.9 MeV·fm^5, x_2=1.425, t_3=15595 MeV·fm$^{(1+\alpha)*3}$ and x_3=0.6044, respectively. The density dependence and the spin-orbit coupling are taken to be α=1/6 and W_0=105 MeV·fm^5. The first two-terms in eq. (1) are the most important for the saturation properties, and the momentum dependent terms are introduced to take into account the effect of the finite-range force and are important for the surface properties. The latter gives rise to an effective mass of m*/m=0.7 in nuclear matter. The strength of the spin-orbit coupling is determined from the energy splitting of $1p_{1/2}$ and $1p_{3/2}$ states in ^{16}O.

Let us now discuss our prescription for the shell-model calculations of the s-d shell nuclei. We first calculated the single-particle energies (s.p.e.) and the two-body matrix elements in ^{16}O and ^{40}Ca. The difference between the H-F and experimental s.p.e. are -2.9 , -1.6 and -0.7 MeV for the $1d_{5/2}$, $1d_{3/2}$ and $2s_{1/2}$ states in ^{16}O, respectively, and 0.0, 0.0 and 1.4 MeV for the holes in ^{40}Ca. We adopted the experimental s.p.e. for the following open-shell calculations. Next, we extrapolated these s.p.e. and two-body matrix elements to other s-d nuclei by assuming a linear mass number dependence through the s-d shell. To check this approximation, we also performed the H-F and two-body matrix element calculations for some other s-d shell nuclei. The difference between the two evaluations was small.

The results of shell-model calculations for low-lying states of the s-d shell nuclei are shown in Figs. 1 and 2. We do not show the excited 0^+ states, such as the state at E_x=3.63 MeV in ^{18}O, which have a large core-excited many-particle many-hole configuration. In Fig. 1, the calculated first 2^+ states both of ^{18}O and ^{36}Ar appear very close to the experimental energies. The first 4^+ and the second 2^+ states are also close to the

experimental ones. Moreover, the excitation energies of the isovector (T=1) states in ^{36}Ar are also reproduced well. The overall agreement between our calculation and experimental data is almost as good as that obtained by Wildenthal [8]. In the latter case, all two-body matrix elements and single-particle energies are determined by a least square fit to the data, while we have no free parameter except those in the interaction (1) which has been previously determined [5]. The 0^+ and 2^+ states of several other nuclei are shown in Fig. 2 in comparison with experiment. Again, the first 2^+ states are in good agreement with experiment except for ^{20}Ne. This discrepancy might be due to the strong deformation in ^{20}Ne which is clearly seen in its rotational-like spectrum. On the other hand, our calculation shows a spectrum with mixed rotational- and vibrational-like features perhaps because of the small configuration space (i.e., one major shell). Our calculations show particularly good agreement with the experimental spectra in the middle of the sd shell such as those for ^{32}S and ^{34}S, both for the isoscalar and higher-lying isovector states.

In order to study more details of our interaction, some two-body matrix elements for the s-d shell configurations are given in Table 1 together with those of Wildenthal [8] and Schiffer and True [7]. We can see a large cancellation between the first two terms of eq. (1) for every matrix element reflecting the attractive and repulsive characters of two forces which are necessary to obtain the proper saturation. The momentum dependent term is always repulsive and behaves like an anti-pairing force. The two-body spin-orbit interaction has an isovector character and is also repulsive for the pairing matrix element. Summing up all four contributions in Table 1, our two-body matrix elements are reasonably close to the phenomenological values given in the last two columns. This is the main reason why our

calculation shows good agreement with the experimental spectra. However, we notice two shortcomings of our matrix elements: (1) the relative strengths of the matrix elements for $(1d_{5/2})^2$- and $(1d_{3/2})^2$-multiplets are very close to the phenomenological values, but the absolute magnitudes are larger; (2) our matrix elements for (J=1,T=0) channel and (J=3,T=0) channel of $(1d_{5/2})^2$ configuration differ significantly from those of Wildenthal. As a result of point (1), our calculated ground state binding energies tend to be too large compared to experimental ones as is seen in Fig. 3.

In the lower part of Fig. 3, we plot calculated root mean square (rms) charge radii of several s-d shell nuclei together with the experimental data. The H-F calculation reproduces well the experimental values at the closed shells within 1% error. The shell-model wave functions give a good account of the mass number dependence of rms radius for the open-shell nuclei. This aspect of our calculation is important for the study of transition densities of excited states.

Arima and his collaborators [9] have claimed that a density-dependent interaction fails to give a realistic spectra at the end of the shell even when it works at the beginning of the shell. However, our interaction gives good agreement in both regions of s-d shell. An important difference between our interaction and that of ref. (9) is the density dependent term. As is seen in Table 1, the two-body matrix elements show a strong cancellation between the δ-term and the density dependent term. Since our force has a lower power for the density dependence, the two-body matrix element has a weak mass number dependence. On the other hand, the three-body force (or equivalently a linear power for the density-dependent term) of ref. (9) has a relatively strong mass dependence and has a much smaller pairing matrix element than ours at the end of the shell.

In order to further investigate the mass dependence, we have also performed the calculations for the Sn-isotopes. Some results are shown in Fig. 4 and compared with experimental data. We use the generalized-seniority scheme [10] for these calculations, taking five single-particle states ($3s_{1/2}$, $2d_{3/2}$, $1g_{7/2}$, $1h_{11/2}$ and $2d_{5/2}$) for the neutron configurations. The H-F single-particle energies give the quasi-particle excitations in ^{115}Sn at Ex=0.0 MeV for $3s_{1/2}$, 0.45 MeV for $1g_{7/2}$, 0.52 MeV for $2d_{3/2}$, 1.10 MeV for $1h_{11/2}$ and 1.30 MeV for $2d_{5/2}$, while the experimental ones are 0.0 MeV, 0.61 MeV, 0.50 MeV, 0.71 MeV and 0.99 MeV for these five particle. For the structure calculations discussed below, we have lowered the $h_{11/2}$ s.p.e. by 400 keV. The energy gaps between the 0^+ and 2^+ states are well reproduced by the calculations for all mass numbers. The best agreement occurs in ^{120}Sn where the second and third 0^+ and 2^+ states are also very close to experiment. Although the 3^- states are always higher than experiment, this is reasonable since the higher $1\hbar\omega$ and $3\hbar\omega$ configurations are important for this collective state. We show some matrix elements for ^{116}Sn in Table 2 together with those of the surface δ-interaction [10]. We obtain reasonable matrix elements not only for the s-d shell configurations but also for the Sn-isotopes without any parameter change.

In summary, we have studied the shell-model calculations for the s-d shell nuclei and Sn-isotopes using the two-body matrix elements of the Skyrme force SGII. Our calculations give good agreement with experimental data in both mass regions without changing any parameter of the interaction. The lower power of the density dependent (α=1/6) force is important to obtain realistic energy spectra both in the beginning and the end of the sd

shell. It would be interesting to apply our interaction to nuclei in other mass regions.

Acknowledgments

We would like to thank A. Arima for enlightening discussions. This work is supported financially by National Science Foundation grant no. PHY-83-12245.

References

1) T. T. S. Kuo and G. E. Brown, Nucl. Phys. 85 (1966) 40

2) G. H. Hering and T. T. S. Kuo, Nucl. Phys. A181 (1972) 113

3) D. Vautherin and B. M. Brink, Phys. Rev. C5 (1972) 626

4) L. Zamick, Proc. of Int. Conf. on Nucl. Structure and Spectroscopy (Amsterdam, 1974) 24

5) Nguyen van Giai and H. Sagawa, Phys. Lett. 106B (1981) 379

6) M. Waroquier et al., Nucl. Phys. A404 (1983) 298

7) J. P. Schiffer and W. W. True, Rev. Mod. Phys. 48 (1976) 191

8) B. H. Wildenthal, Progress in Particle and Nuclear Physics, Vol. II (1983) p.5, and private communications

9) T. Inoue et al., Proc. of the Int. Conf. on Nucl. Structure Vol. I (Amsterdam, 1982) p.318

A. Arima, Invited talk at Int. Conf. of the Shell Model Theory (Philadelphia, 1984) and private communications

10) I. Talmi, Nucl. Phys. A172 (1972) 1

O. Scholten, Phys. Rev. C28 (1983) 1783

11) Table of Isotopes (John Wiley & Sons, Inc., 1978, edited by C. M. Lederer and V. S. Shirley)

12) A. H. Wapstra and K. Bass, Atomic Data and Nuclear Data Tables 19 (1977) 177

13) B. A. Brown et al., J. Phys. G: Nucl. Phys. 10 (1984) 183

14) L. J. Tassie and F. C. Baker, Phys. Rev. 111 (1958) 940

15) A. Bohr and B. R. Mottelson, Nuclear Structure, Vol. I (New York, Benjamin Inc., 1975) p.380

16) P. J. Brussaard and P. W. M. Glaudemans, Shell-model Applications in Nuclear Spectroscopy (North-Holland Pub. Co., 1977) p.106

Figure captions

Fig. (1) Calculated and experimental energy spectra of ^{18}O and ^{36}Ar. The data are taken from ref. (11).

Fig. (2) Calculated and experimental energy spectra of various s-d shell nuclei. The data are taken from ref. (11).

Fig. (3) Calculated and experimental binding energies and rms charge radii of s-d shell nuclei. The data for binding energies are taken from ref. (12), while the data for rms radii are the references given in [13]. The difference between the shell-model and the H-F calculations for binding energy in ^{40}Ca stems from the shift of the $2s_{1/2}$ s.p.e. in the shell-model calculation. The center-of-mass correction for the rms radius is taken into account in the harmonic oscillator model [14] and the nucleon finite size correction is incorporated in the dipole approximation [15].

Fig. (4) The energy spectra of Sn-isotopes. The data are taken from ref. (11).

Table 1. Two-body matrix elements for some sd shell configurations. The phenomenological values are taken from ref. (8) (W) and ref. (7) for (S-T).

	J	T	δ	$\rho^{\alpha}\delta$	$\vec{k}^2+\vec{k}'\cdot\vec{k}$	$\vec{L}\cdot\vec{S}$	SGII	W	S-T
	1	0	-15.55	9.33	2.26	0.	-3.96	-1.63	-3.3
	3	0	- 8.73	5.24	1.04	0.	-2.46	-1.50	-1.6
$(1d_{5/2})^2$	5	0	-13.65	8.19	0.83	0.	-4.63	-4.22	-3.7
	0	1	-23.92	15.23	4.35	0.63	-3.72	-2.82	-3.2
[^{16}O core]	2	1	- 5.47	3.49	0.52	-0.34	-1.80	-1.00	-0.9
	4	1	- 2.23	1.45	0.01	-0.09	-0.90	-0.16	0.3
	1	0	- 8.13	5.36	0.82	0.	-1.96	-1.13	-2.2
$(1d_{3/2})^2$	3	0	- 8.13	5.36	0.38	0.	-2.40	-2.30	-2.7
	0	1	-11.32	7.91	1.44	0.53	-1.45	-1.75	-2.9
[^{40}Ca core]	2	1	- 2.26	1.58	0.18	0.04	-0.47	-0.05	0.2

Table 2. Two-body matrix elements in the Sn-region. The coupling constant of the surface δ-force [16] is taken to be A_T=0.18 MeV[10].

	J	T	SGII	surface-δ
$1g_{7/2}$	0	1	-0.73	-0.72
	2	1	-0.39	-0.17
	4	1	-0.21	-0.08
	6	1	-0.13	-0.04
$2d_{5/2}$	0	1	-0.66	-0.54
	2	1	-0.44	-0.12
	4	1	-0.23	-0.05

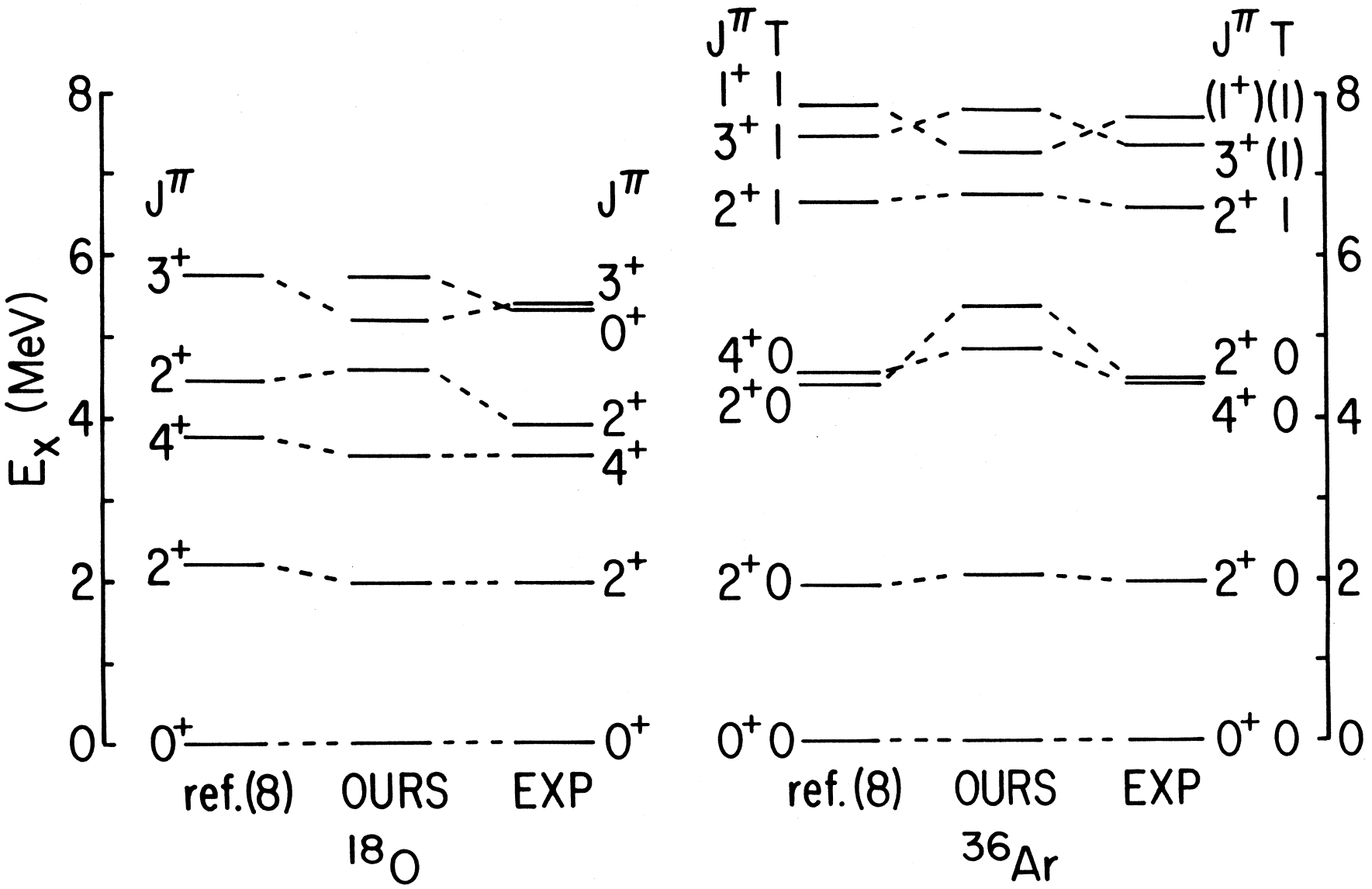
E_x (MeV)
8
6
4
2
0
J^π
3^+
2^+
4^+
2^+
0^+
3^+
0^+
2^+
4^+
2^+
0^+
0^+
ref.(8)
OURS
EXP
^{18}O
J^π T
1^+ 1
3^+ 1
2^+ 1
4^+ 0
2^+ 0
2^+ 0
0^+ 0
$(1^+)(1)$
$3^+(1)$
2^+ 1
2^+ 0
4^+ 0
2^+ 0
0^+ 0
ref.(8)
OURS
EXP
^{36}Ar

FIGURE 1

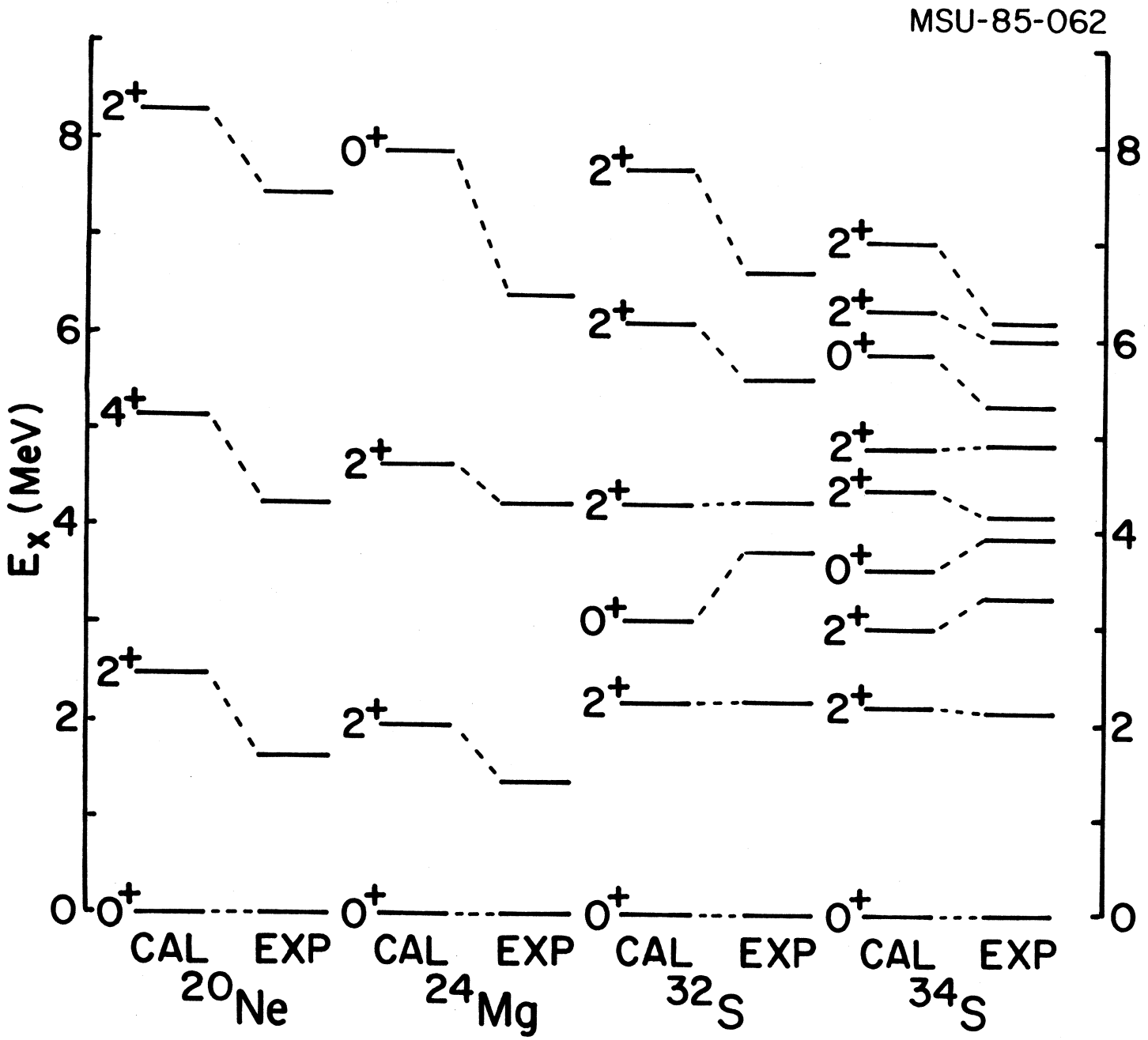

FIGURE 2

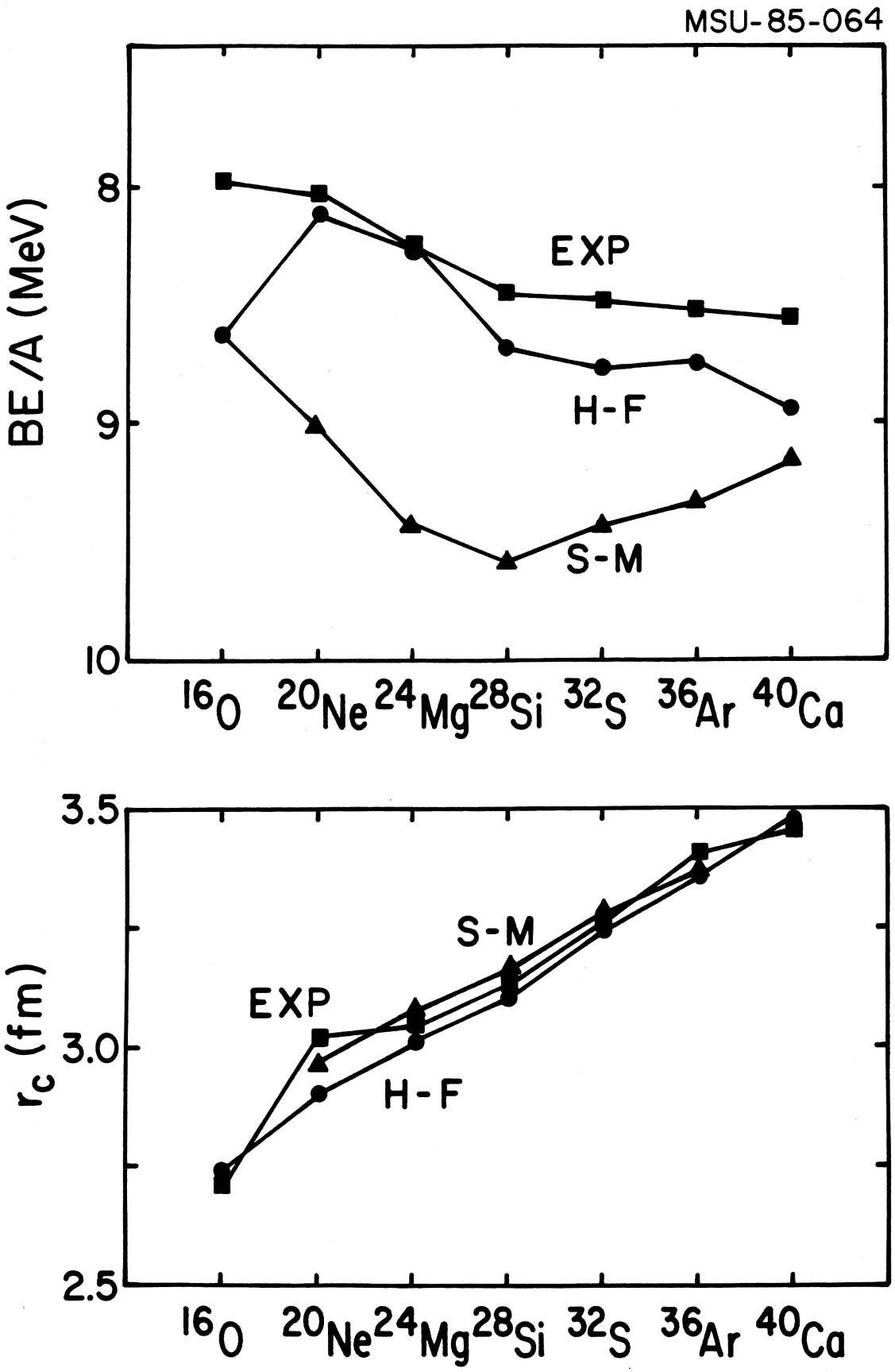
MSU-85-064
BE/A (MeV)
8
9
10
EXP
H-F
S-M
16O 20Ne 24Mg 28Si 32S 36Ar 40Ca
rc (fm)
3.5
3.0
2.5
S-M
EXP
H-F
16O 20Ne 24Mg 28Si 32S 36Ar 40Ca

FIGURE 3

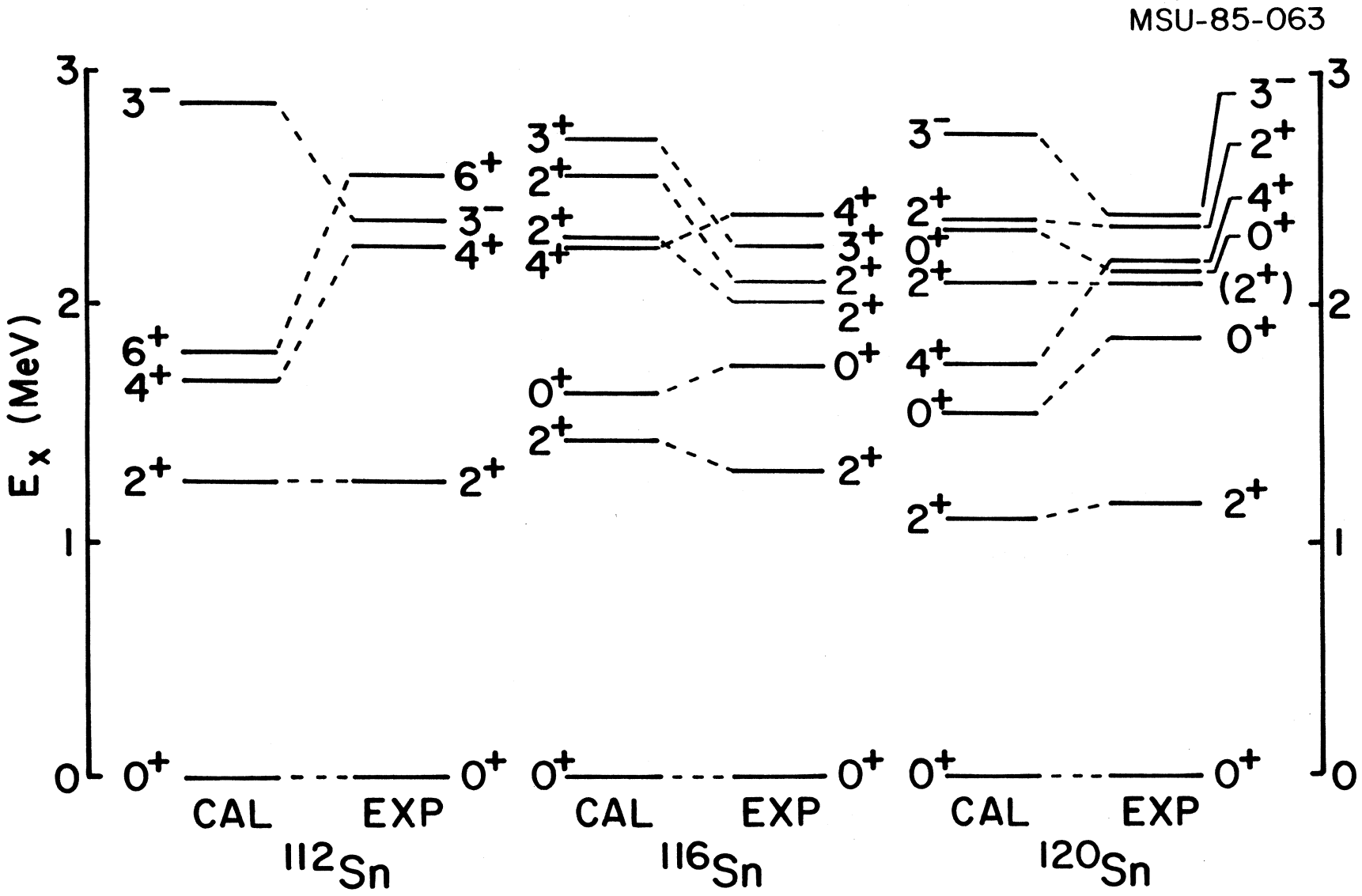
MSU-85-063
E_x (MeV)
3
2
1
0
3^-
6^+
4^+
2^+
0^+
3^-
4^+
2^+
0^+
CAL
EXP
^{112}Sn
3^+
2^+
2^+
4^+
4^+
3^+
2^+
2^+
0^+
2^+
0^+
2^+
0^+
CAL
EXP
^{116}Sn
3^-
2^+
0^+
2^+
4^+
0^+
2^+
3^-
2^+
4^+
0^+
(2^+)
0^+
2^+
0^+
CAL
EXP
^{120}Sn

FIGURE 4